Smithsonian

Contributions to Astrophysics

Volume 3, Number 6

A FLUID-DYNAMIC MECHANISM OF METEORITE PITTING

by David T. Williams

SMITHSONIAN INSTITUTION
Washington D.C.
1959

Publications of the Astrophysical Observatory

This series, *Smithsonian Contributions to Astrophysics*, was inaugurated in 1956 to provide a proper communication for the results of research conducted at the Astrophysical Observatory of the Smithsonian Institution. Its purpose is the "increase and diffusion of knowledge" in the field of astrophysics, with particular emphasis on problems of the sun, the earth, and the solar system. Its pages are open to a limited number of papers by other investigators with whom we have common interests.

Another series is *Annals of the Astrophysical Observatory*. It was started in 1900 by the Observatory's first director, Samuel P. Langley, and has been published about every 10 years since that date. These quarto volumes, some of which are still available, record the history of the Observatory's researches and activities.

Many technical papers and volumes emanating from the Astrophysical Observatory have appeared in the *Smithsonian Miscellaneous Collections*. Among these are *Smithsonian Physical Tables*, *Smithsonian Meteorological Tables*, and *World Weather Records*.

Additional information concerning these publications may be secured from the Editorial and Publications Division, Smithsonian Institution, Washington, D.C.

FRED L. WHIPPLE, *Director,*
Astrophysical Observatory,
Smithsonian Institution.

Cambridge, Mass.

For sale by the Superintendent of Documents, U.S. Government Printing Office
Washington 25, D.C. - Price 65 cents

A Fluid-Dynamic Mechanism of Meteorite Pitting

By David T. Williams [1]

The study of meteorite pitting is one part of the broader subject of meteor (and meteorite) ablation which has been investigated for many years. A large number of such studies have dealt primarily with meteor data obtainable by photographic and spectrographic methods, and with analyses designed to aid in interpreting the results (Whipple, 1943, 1955; Whipple and Thomas, 1951; Cook, 1954; Cook, Eyring, and Thomas, 1951; Smith, 1954; Thomas, 1952; Thomas and Whipple, 1951; Thomas and White, 1953).

Reasonable and simple theories have been developed for relating the brightness of meteors to their masses. These data have been of use in determining the density of air in the upper atmosphere at heights between 40 and 120 km. The details of the processes of ablation of material from meteor surfaces have been of particular concern. Present opinion appears to be that meteors are sometimes broken up as they enter the atmosphere (Jacchia, 1955); that meteorites exhibiting unsteady brightness (or flaring) emit very small particles of the order of 10^{-7} grams, in bursts (Smith, 1954); and that nonflaring meteorites ablate by vaporization rather than by melting (Cook, 1954). The spectrum of a Perseid meteor shows the presence of atomic spectral lines that support this conclusion (Cook and Millman, 1955).

Data on ablation supplementing those obtained by meteor trail photography have accumulated from experiments using high-speed pellets (Allen, Rinehart, and White, 1952; White, Rinehart, and Allen, 1952; Rinehart, Allen, and White, 1952). Light from the wake of such bodies shows lines of the elements in the pellet, as well as bands of the oxides of those elements. In some cases at least, the pellet trails show a flashing phenomenon concluded to result from yawing of the pellet. The light has been identified as coming both from the shock front and from the trail (Allen and Mayfield, 1953; Thomas and White, 1953; White, 1955). The ablation processes acting on meteors, where very small solid objects are acted upon by relatively rare gases in the upper atmosphere, have received particular study. Of special interest has been the relation of such processes to the ablation of the larger meteorites that penetrate the denser layers of the atmosphere without complete disintegration. Some experiments on high-speed pellets have been made to correlate the ablation processes with the resultant shapes of the partly ablated bodies (Whipple and Thomas, 1951; Whipple, private communication).

Surface features of meteorites

The nature of the surface features of meteorites has particular interest. Many rather complete descriptions of the surfaces of meteoritic stones and irons are in the literature (e.g., Henderson, 1958; Nininger, 1936a, 1936b, 1952). Outstanding among commonly observed surface features are evidences of eroding airflow: flow lines in surfaces of some stone or iron meteorites with clearly recognizable stagnation points; frangible crusts of material on some meteorites so obviously congealed from the molten state as to require no further proof; shapes that strongly suggest carving by the action of airflow over the surface. (Pictures are shown in Nininger, 1952, pls. 31–33, 40–43.) Not all meteorites, however, show such clear evidence of airflow on their surfaces. Another phenomenon, which also is common without being

[1] University of Florida, Gainesville, Fla.

universal, is that pits appear in the surfaces of meteorites, both stone and iron. Nininger (1952) and Henderson (1958) have discussed these features.

The question whether a direct relation exists between the pits in meteorite surfaces and the ablating action of the air on them has been answered by Nininger in one way and by Henderson in another. Nininger apparently has concluded that the pits are caused by selective melting in surfaces that are not chemically homogeneous. This conclusion is in itself moderately clearcut. Nininger also suggests, however, that turbulence of the air flowing into and around the pits tends to deepen them. Again he remarks (Nininger 1952, p. 180) that in certain quite inhomogeneous meteorites (Pasamonte, Allegin, and Estherville) no pitting is observed, while some homogeneous meteorites are deeply pitted (Rosebud stone). Finally, from the frequency of pitting in relation to the probable speed of fall, Nininger generalizes that pitting is observed more often in the faster flying bodies. The selective melting of meteorites is still concluded to be the mechanism of pitting, evidence relating to the homogeneity of pitted bodies to the contrary notwithstanding.

Henderson (1958) points out that many cavities are too intricate or deep to have been reasonably caused by airflow. Some cavities might have resulted from influences unspecified in the early life history of the bodies. Henderson also speculates on the effect of "wave action" on cavities, and on possible aerodynamic or thermal mechanisms of formation.

The opinions of Nininger and Henderson are not necessarily in conflict, in view of the variety of phenomena to be observed on meteorite surfaces. Obviously, however, there is room for more evidence on the relation between ablation and pitting. The present paper is designed to present such evidence.

Flow patterns on "oriented" meteorites

It is a characteristic of Nininger's (1936a, 1936b, 1952) work that he has deduced the manner of the airflow over meteorites by direct observation of flow lines in the surface. Rinehart (1957) has made a similar study. This technique has been recognized as useful for many years (e.g., Riabouchinsky, 1909; Fales, 1926) but it has not yet been entirely exploited. Detailed analyses have not been made of directions of airflow over the surfaces in question so as to identify in detail not only the nature of the airflow but the mechanism by which the flow might have caused the surface peculiarities of meteorites during their flight through the atmosphere. That type of analysis is presented here.

The work began in 1957 under the sponsorship of the Army Ballistic Missile Agency at Huntsville, Ala., while the author was at Battelle Memorial Institute in Columbus, Ohio. It has been continued at the University of Florida at Gainesville, with some support from the Engineering Experiment Station of that institution and from the Smithsonian Astrophysical Observatory in Cambridge, Mass.

A word of caution may be appropriate at this point. The study of flow patterns produces data relating to the boundary layer of airflow over solid bodies. Such data are peculiarly pertinent to ablation since melting occurs strictly at the surface; but description of the flow pieced together from such data is far from complete. The investigator must rely heavily upon insight gained by experience in aerodynamics in order to interpret and supplement his direct observations. He must use his imagination, and by that very act he risks being challenged by other scientists whose insights are based on other disciplines.

In order to meet possible skepticism on the part of other investigators in this field, the present study is supported by many unusually revealing photographs. The hope is that the reader may be convinced by the evidence of his own senses insofar as insight is required to interpret the data, and that thereby he may reach the same conclusions as has the author.

Flow patterns from a rocket blast

An unusual feature of flow patterns on meteorites is the fact that the flow speed is initially supersonic. Whether this circumstance would have any important effect on the flow patterns might be questioned. An experiment involving erosion of a simple model by initially supersonic flow was therefore arranged in order to discover what might be anticipated under more complex conditions.

Plate 1 shows the erosion pattern carved on the flat surface of a ceramic sample by the blast of an oxygen-hydrogen rocket, incident at an angle of 30° from the surface. The rocket had a chamber pressure in excess of 100 psi; the convergent nozzle was a slit one-eighth inch by 1 inch in cross section, the long dimension being parallel to the plate. Apparently the blast eroded the plate by melting, carrying streamers of glassy material straight along the plate in its main flow but diverging slightly from the point of initial impact. The flow beneath and around the main stream was somewhat more intricate. The erosion was not regular, but was especially intense at certain points ("A" and "B" in fig. 1) as though the flow had "bounced"

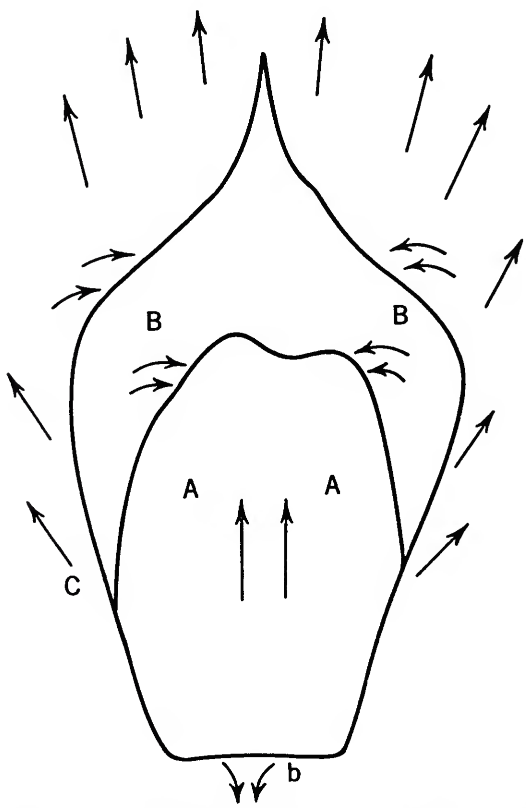

Figure 1.—Schematic version of erosion in a ceramic plate caused by a rocket blast (see pl. 1). Solid lines indicate vortex flow in the lee of crests; arrows, flow lines; "A" and "B", areas of intense erosion; "b", region where gas flow was reversed; "C", crest.

on the surface, or induced waves on it. At point "b" (fig. 1) the flow was directly reversed, carrying glass filaments in a direction opposite to the main flow. Plate 2*a* shows an enlargement of region "b." The filaments terminate in blobs of glass (rounded by surface tension of the molten glass), indicating the sense of the airflow.

Region C (fig. 1) is shown enlarged in plate 2*b*. At this point the erosion pattern has a "crest," like that of a wave about to break. The crest overhangs the plate beneath. A vortex is assumed to lie in the lee of the crest, scrubbing its downstream side and lifting it above the plate. The air that scrubbed it obviously left the surface of the sample at the crest.

The crest at "C" extends along the plate and veers over toward the center of the plate. An enlarged photograph (pl. 3) of the region just upstream of "B" (fig. 1) provides evidence of the nature of the flow in the lee of the crest. At the point shown the vortex was a left-hand spiral. Air from the vortex would leave the crest at its top on the downstream side, joining the main flow over the crest from the upstream side. A crest showing a sharp edge and evidence that glass was pulled off the solid edge (as in pl. 2*b*) is sometimes referred to as a "skirt" in the following paragraphs.

Figure 1 and plates 1 to 3 are not intended to prove any explicit characteristics of airflow around meteorites. The flow in the experiment was from a jet of small size onto a plate initially flat. Air was drawn into the jet from the atmosphere, and its characteristic flow pattern is obviously different from that over any real meteorite. On the other hand, the photographs do provide valuable insight for use in interpreting flow patterns on meteorites. The following specific conclusions may be drawn:

(a) A straight flow over a flat surface produces erosion that is not necessarily uniform, even though the flow may be supersonic.

(b) A flow that is initially supersonic becomes subsonic in the boundary layer. Its direction may be at right angles to or even directly reversed from that of the main supersonic flow.

(c) At a region where the main flow tends to leave the surface (at a crest or skirt), a vortex is to be anticipated in the lee of the crest.

It is notable that the flow in a boundary layer, in this experiment, showed the same qualitative characteristics when the flow outside the layer was initially supersonic as it would be expected to show below a subsonic flow.

The Estherville meteorites

Nininger (1936b, 1952) has described the small iron meteorites of the Estherville fall and has published pictures of some of the specimens. Photographs of some of these meteorites (pl. 4) were taken by the author at the Peabody Museum at Yale University. In order to bring out the fine detail of the flow patterns, the surfaces were smoked by use of burning magnesium ribbon. Illumination was from the side at a grazing incidence.

Plate 4*a* shows an Estherville oriented meteorite with a smooth iron surface, coated with a frangible oxide crust which bears a fine tracery of flow lines. The smooth iron can be seen near the top where the crust has been broken off. The stagnation region is at the center of the picture, and the direction of airflow was roughly upward. (Note: The term "stagnation region" or "stagnation point" is applied to the area on the leading surface from which all flow lines diverge.)

The meteorite pictured in plate 4*b* shows evidence that the iron was once molten; it has the form of a congealed flow like candle wax.

The meteorite pictured in plate 4*c* also shows evidence of having been bathed by a flow of molten iron. The appearance of the oxide layer strongly indicates that its flow was more or less independent of that of the iron beneath. There is striking evidence that the oxide layer actually flowed off the irregularities of the iron flow, as though the iron had congealed somewhat before the oxide. It is interesting in this connection to observe that pure iron melts at 1535° C; FeO melts at 1420° C, a temperature some 100° lower. Thus, a layer of FeO might conceivably still have been molten on freshly congealed iron. (The fact that the iron in meteorites is not pure is presumed not to affect this conclusion.) The oxide Fe_2O_3 has a melting point of 1565° C. One would expect to find a thin dust of Fe_2O_3 floating on the layer of FeO at the time when the latter congealed. Whether this is in fact the case cannot be determined clearly from these pictures.

The pictures shown here demonstrate the types of flow lines that may be visible on meteorite surfaces. When present, they provide clear evidence of the direction and sense of air flow. They may reveal the occurrence of phenomena, not at first anticipated, during the atmospheric flight.

The Lafayette meteorite

The delicate structure of the flow lines in iron oxide on the Estherville irons is in marked contrast to that of the flow lines in some of the oriented stony meteorites. An example of the latter is the Lafayette meteorite (USNM 1505) at the U.S. National Museum. This stone (pl. 5) is roughly hemispherical in shape, some 10 cm in original diameter, with a smooth rounded surface and a flat back (Nininger, 1952). A portion of the original stone was sectioned off and is missing.

The Lafayette meteorite was photographed by use of an ammonium chloride smoke rather than the magnesium oxide used on the irons. The black color of the meteorite is not altogether concealed in plate 5*a*; there are regions on the right where it shows through. Smooth glazed ridges diverge from the stagnation region on this specimen as rivulets of black slag. The dimensions of these features appear to be uniform from the stagnation region to the edge of the front face but as the distance from the stagnation point increases these rivulets possibly are slightly higher than near where they originate. Also they become more numerous near the edge of the forward face. The flow pattern strikingly resembles that on a windshield of a car moving at high speed in the rain.

A relatively heavy deposit of slag, carried by the wake ring vortex, is to be seen in a broad region at the center of the trailing face (pl 5*b*). This material is full of holes, as though gas were being evolved in it at the time when it congealed. The color and luster of the slag on the rear face are different from the glass on the forward side of the meteorite.

Out toward the margin of the rear face there is unmistakable evidence of flow, roughly radial from the central region. The sense of the flow is indicated by points where threads of slag were apparently drawn off outward. At the margin itself, the slag looks as though it had been spun off in threads and droplets by the joining of airflows from the front and rear surfaces.

Reconstructing the pattern of airflow around the Lafayette meteorite is reasonably simple. Obviously, the air streamed straight along the front surface, melting the stone in a thin layer of slag and sweeping the slag back in straight lines. At the edge between front and rear, the flow from the front left the stone, carrying with it slag from the front surface. In the region behind, a doughnut-shaped vortex was formed by the flow, in the manner suggested in the sketch (fig. 2). By some mechanism, possibly

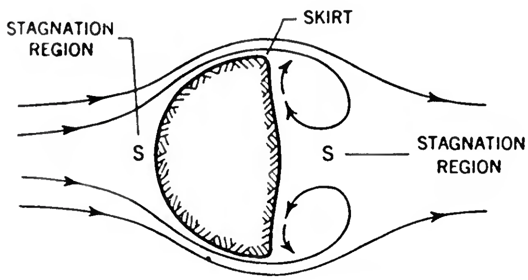

FIGURE 2.—Flow pattern around the Lafayette meteorite as deduced from the markings on the surface. The trailing ring vortex is shown in section as two vortices behind the stone.

the same vortex, some of the slag was spun off from the skirt at the margin of the stone and deposited at the center of the back face. The holes in the slag layer might be due to air that was absorbed during flow across the front face, and released in the relatively low pressure in the lee of the stone.

According to this interpretation, the airflow out toward the margin of the trailing face tended to accelerate, carrying slag along in rivulets. At the edge, air and glass were swept off by the strong flow from the front face, leaving some slag behind in the form of the skirt.

It must be recognized that the picture sketched in this fashion is not the only conceivable one. The conclusion that air leaves the surface of the meteorite at the skirt is believed to be much more reasonable than the assumption that air might actually follow the surface around a sharp edge. This also sometimes happens, as will be made clear later, but when it does there is no skirt such as is to be seen around most of the margin of the Lafayette meteorite (pl. 5*b*). Furthermore, the appearance of the flow lines about half way to the margin, as revealed on a glossy print, is compatible only with the hypothesis that flow is toward the margin rather than away from it.

The Plainview meteorite

The conclusions relating to the airflow around the Lafayette stone are strengthened by the results of a study (Henderson and Williams, 1958) of another oriented stone, the Plainview meteorite (USNM 521). It appears to have been altered to only a moderate degree by the airflow in its flight through the atmosphere. Plate 6*a* is a photograph of the front face of this meteorite. The specimen is a block, shaped roughly like a keystone. The sides to the left and lower left of the figure form an obtuse angle with the face itself, and are therefore scrubbed directly by the main airflow. The sides at the top and right of the figure are undercut. Being shielded from the direct flow, they were washed by a reversed flow from the back due to a ring vortex in the rear of the body.

The sketch (fig. 3*a*) shows the airflow across the face as deduced by observation of the flow pattern. The flow lines on the front face (pl. 6*a*) are easily traced on a glossy print either with or without a hand lens.

In flight, the leading face was tipped perhaps 20°, the left side being ahead of the right. A group of shallow pits (in upper right of pl. 6*a* and indicated by "2" in fig. 3*a*) terminate in a high hornlike projection. In these pits, flow lines are seen diverging from a stagnation region at the center. In the side of the pit nearest the main stagnation point, the flow from area "2" in figure 3*a* scours the edge of the pit. The main flow from "S" leaves the surface of the stone at the crest shown by the broken line. Apparently there is actual scrubbing of the inner walls of the pit. The mechanism by which the air can flow in opposite or nearly opposite directions on either side of a crest is, presumably, a helical vortex inside the pit with axis parallel to, and just downstream of, the crest.

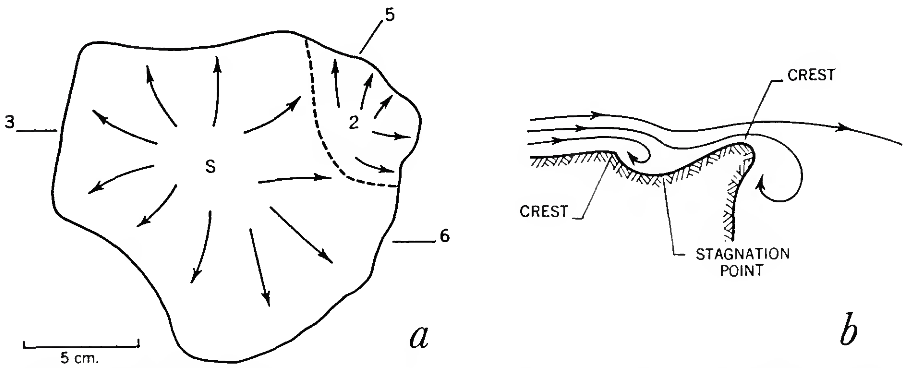

FIGURE 3.—Flow patterns around the Plainview, Tex., meteorite. *a*, Leading face: Broken line shows crest; arrows in shallow pits (2) on right indicate flow lines; larger arrows, flow pattern from the main stagnation point (S); numbered areas (3, 5, 6) are those pictured in plates 11, 13, and 14 (respectively). *b*, Pit shown in area "2" of *a* and in plate 10; vortex is shown in section at the deepest portion of the pit, lying just to the lee of the crest.

The flow in the pit is indicated in figure 3*b*. The vortex shown in the pit is ascribed to the aspirating action of the main flow, which generates a relative vacuum in the pit. In reaction, the airflow across the pit is pressed down by the higher pressure outside, to impinge again on the stone surface. This impingement, with the vortex, forms a stagnation region inside the pit, with airflow diverging outward radially toward the crest around the depression.

Plate 6*b* shows the side of Plainview No. 521 that appears on the left in plate 6*a* ("3" in fig. 3*a*). Evidence indicates that this side is exposed to direct airflow. The pits over the entire surface are clearly seen to be scoured by the air. The downstream sides of each pit show flow lines diverging more or less radially from the deepest part. Usually the flow marks are less clear on the inside of the pit nearest the main upstream direction. In the intricate shapes on the left of the figure, there is evidence that molten material has flowed from the bottom of some pits and deposited on the edge on the downstream side. This region was apparently enough sheltered from the main airflow so that the crests on the downstream side of the pits were not swept as clear of slag as in more exposed areas. The solid glass looks here like the wavelets on a beach at the point and moment of the furthest advance of a breaking wave. The parallel between appearance of the slag and the form of waves is, of course, not altogether accidental.

The mottled appearance of the trailing face (pl. 6*c*) of Plainview No. 521 is due to the presence of broad, shallow depressions, and is strikingly typical of trailing faces of bodies eroded by any fluid flow. The streamers of slag radial from the center of the face are quite different in appearance from those on the leading face; there are fewer of them, and they tend to lie straight across the surface irregularities instead of being turned or reversed as was found in the front surface pit of plate 6*a*. No evidence of bubbling is found here, such as appears on the trailing face of the Lafayette meteorite.

The edge of the trailing face shown in plate 6*c* would be expected to be the location of a skirt, if the Lafayette stone (pl. 5*b*) is a reasonable criterion. In contrast, however, Plainview No. 521 (pl. 6*c*) shows a skirt over less than half of the periphery of the trailing face. On the edge to the left there is a skirt as far around as the point at the bottom. The rest of the edge is smoothed, indicating neither crest nor skirt, although the edge is a region of sharp change in plane orientation. The nature of the airflow across this edge is clarified in figure 4*a* and in plate 7*a*,*b*.

The question has been posed whether the slag deposited on the back face of meteorites may not have resulted from the deceleration of the meteorite, the slag in the wake making a rear-end collision with the stone. Such a mechanism, however, would apparently not change the nature of the conclusions regarding

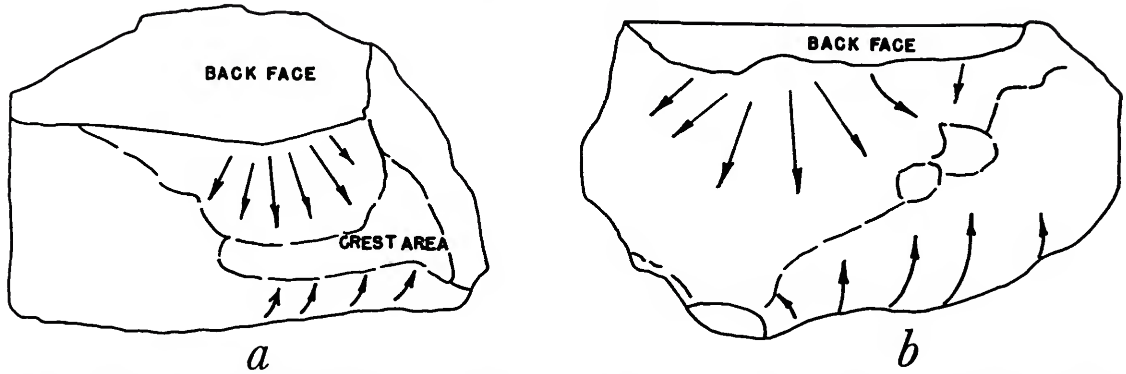

FIGURE 4.—Sketches of sides of the Plainview, Tex., meteorite. *a*, Side 5 shown in plate 13: This face was in the lee of the relative wind, so that airflow left the surface near the bottom and formed a crest roughly along the broken line; the trailing face in this region showed no edge skirt, confirming the interpretation made here. *b*, Side 6 shown in plate 14: Location of the crest region near bottom of this face is readily accounted for by presence of the projection there;[3] the flow was forward, induced by the trailing vortex system behind the stone.

the airflow around the meteorite. Thus, in still air the deceleration $-dv/dt$ of any object of given shape would increase as its size decreased, because the drag would decrease as its diameter squared, whereas its mass would decrease as its diameter cubed. That is,

$$-\frac{dv}{dt} \propto \frac{d^2}{d^3} \text{ or } \propto \frac{1}{d}.$$

Here d is the diameter. This means that slag particles could overtake the parent meteorite only if the air in the wake had some forward velocity. As shown in plate 6*c*, the air must have had enough forward velocity actually to overtake the stone, i.e., to form a trailing toroidal vortex, for there is a stagnation point at the center of the face and there are streamers of slag radial from that point.

If small particles of slag can overtake the stone because of its deceleration in flight they might conceivably be observed as solid chunks which had time to congeal before striking and sticking to the back face. Furthermore, they would presumably be more widely distributed in the point of impact than would slag drawn along primarily by the trailing toroidal vortex.

On careful examination of the photographs of the front (pl. 6*a*) and back (pl. 6*c*) surfaces, small particles of material are seen that look as though they might indeed have been deposited directly on the surfaces, in the solid state. The distribution of the particles is more or less random, and the little heaps of material are larger in size on the back face than on the front. Mr. E. P. Henderson, associate curator of mineralogy at the U.S. National Museum, examined these particles and concluded they are pieces of sand stuck to the surface by alterations that occurred after the meteorite had fallen to the ground. It therefore is concluded that even granting the possibility of solid slag particles overtaking the meteorite in flight, no data supporting such a speculation have been identified by this author.[2]

The presence of a sharply overhanging region on the side of the meteorite has been mentioned. Observe the flow on side 5 in figure 3*a* (shown also in pl. 7*a* and sketched in fig. 4*a*). This side was enough behind the stone so that the airflow broke away near the bottom of this face. In plate 7*a*, the heavy slag deposit was scoured forward from the trailing face. The shadowed region at the top is the back face of the stone. In the center of the picture, sharply etched flow lines diverge downward from the

[2] Note added in proof: Mr. Henderson has forwarded to the author a picture of the trailing face of the Pasamonte, New Mexico, meteorite. This picture shows droplets of once-molten slag that would seem to have been carried away from the edge of the stone and been redeposited on its rear by the trailing vortex in the wake behind the meteorite. It is not altogether clear from this photograph that the droplets were free of the stone, rather than streamers from the skirt, when the deposition occurred. Furthermore, flow lines revealing any significant detail of the air currents across this face do not show in the photograph, if they are in fact present. It is nevertheless concluded by this author that slag may be deposited from the wake after enough cooling has taken place to cause some degree of solidification. To what extent deceleration of the parent stone was the proximate cause of the rear-end collision on the Pasamonte stone is a matter on which no conclusion has been drawn here.

back face. These flow lines indicate back flow from the back face toward the front, as can be verified by careful examination of plate 7*a* and of the stone itself. Lines of airflow from the front face toward the back can be seen also at the bottom of the photograph. The airflow collides with that from the trailing face in the region of the crest (shown as a dotted line in fig. 4*a*) where both airflows abruptly leave the stone surface. There is no skirt of slag here because the stone has no sharp edge at the line where the airflow leaves the stone.

It may seem a little surprising, at first, to see such sharply visible flow lines in the lee of a meteorite, indicating reversed flow. They do not necessarily mean that the surface was heavily eroded there; on the contrary, they simply mean that much slag was left by the slow-moving air.

Adjacent to this overhanging side 5 is region 6 of figure 3*a* (shown in pl. 7*b* and also sketched in fig. 4*b*).This region is also overhanging, and lies in the lee of flow over the leading face of the stone, just as for the face shown in figure 4*a* and plate 7*a*. As is to be expected, reversed flow is seen here, with a clearly visible crest area near the bottom, accounted for by the presence of the projection visible at the bottom of the figure. This put the face in the lee of the flow, so that the airflow from the leading face left the surface instead of following it beyond the crest.

Study of the flow patterns on Plainview meteorite No. 521 led to a consistent and rational picture that agrees with the qualitative laws of aerodynamic flow. Airflow over the front face of this meteorite, much like that on the Lafayette, broke away from the body in a crest belt surrounding the stone. The Plainview stone was irregular in shape and tilted a little in the airflow, so that the crest did not coincide at every point with a sharp edge of the stone, to form a skirt. In this respect, the Lafayette and the Plainview specimens apparently differed, but the difference is strictly predictable from the nature of airflow and the shapes of the stones.

The Olivenza fragment

A fragment (in the Peabody Museum at Yale University) from one of the Olivenza, Spain, meteorites was smoked with magnesium oxide and photographed (pl. 7*c*). This heavily pitted fragment of a stony meteorite is surmised to have been originally on the side of the main body, well back from the stagnation region.

The extraordinary clarity of the flow patterns in the pits presumably results from the fact that the region shown was not so vigorously scoured as were areas on the leading face; more slag is left to show how the air flowed. Stagnation regions are visible at the bottom of the pits. Flow lines stream away from the stagnation points in directions more or less normal to the crests around the pits but flying downstream a little with the main wind. As in some of the Plainview pictures, there are many crests where slag has deposited, as though swept up from the bottom of neighboring pits.

The perfect whorl in the center of the picture is unusual in that its axis is normal to the surface rather than parallel to it.

The Miller meteorite

A photograph (pl. 8) of the leading face of the Miller, Arkansas, meteorite (in the American Museum of Natural History) shows how pits in meteorites may be oriented with reference to the stagnation region. Flow lines appear inside the pits as well as elsewhere on the surface. These lines are difficult to see in the photograph because the stone was not smoked before the picture was taken. The pits themselves are clearly arrayed radially around the stagnation region. In shape they are elongated, with their long axes radiating from the stagnation region.

General conclusions

The series of photographs presented here were intended to establish certain general conclusions relating to airflow over the surfaces of meteorites:

(a) The surfaces can bear clear evidence of the nature of airflow over a melting meteorite, stone or iron. When flow lines are found, evidence of the direction of the flow can be persuasive if not decisive, both as to line and sense.

(b) The pattern of airflow as observed is characterized by reversed flow in the lee of bluff objects. A band marking the position of a crest will form a continuous ring around any bluff meteorite shape.

(c) Flow lines inside of pits in the surface indicate a stagnation point at the deepest point, with flow diverging toward the edge of the pits. Such flow might be caused, for example, by a vortex with axis having a hairpin shape, lying in the pit straddling the stagnation point in the pit. The ends of the vortex would then trail off to infinity downstream in the wake, much as the tip vortices of wings in the conventional vortex theory of lift.

There are certain further possible conclusions that the foregoing observations did not establish entirely:

(a) Thus far no clear evidence exists that any pits are of aerodynamic origin, even though the appearance of the Miller meteorite strongly suggests such a mechanism.

(b) In general, the presence of flow lines inside the pits on a congealing meteorite surface proves only that air will flow inside the pits. Since it does, a conceivable mechanism for pit formation exists in the airflow, but the assertion that such a mechanism did actually operate to deepen pits has not been made as yet.

The main point of this discussion is that the conclusions listed above resulted from a study of the flow lines on meteorites; they are precisely what one might have expected from a study of ablation of a body subjected to a subsonic liquid flow. Neither the vortices in the lee of bluff objects nor the reversed flow due to a vortex in a steep-walled depression depend specifically on the supersonic nature of the flow, except insofar as such a flow is required to produce the melting temperatures of stone. The obviously subsonic speed of the flow over meteorites is, of course, not altogether unexpected, since the flow that is mainly effective in producing flow lines is that at the bottom of a boundary layer. The subsonic speed does suggest, however, that one need not be limited to supersonic flows in searching for an aerodynamic mechanism for meteorite pitting.

Erosion of salt cakes

The preceding discussion leads directly to the conclusion that if an aerodynamic mechanism does produce pitting in meteorites, then laboratory experiments should be able to demonstrate a similar pitting in objects subjected to erosion by fluid flow, at subsonic speeds. A program was therefore carried out to investigate in a strictly exploratory manner the erosion in water of salt blocks such as are used in Florida and elsewhere for supplementing the diet of cattle.

Cakes were purchased and mounted on a "stinger," or short iron rod, supported on a framework mounted on the prow of a skiff (see fig. 5). The framework was hinged so that the salt blocks could be immersed or withdrawn from the water while the boat was in motion. The attitude of the blocks and the depth of submersion were adjustable, between runs.

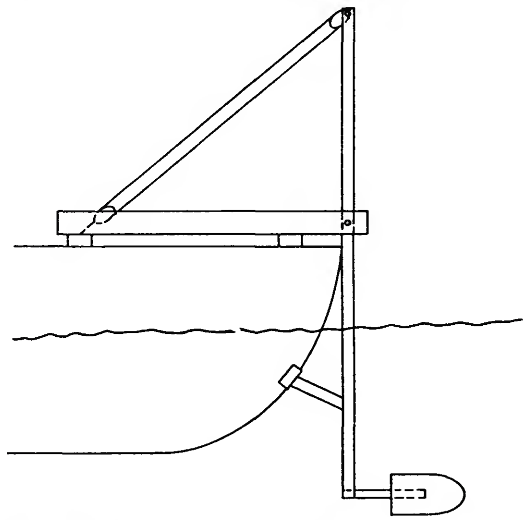

FIGURE 5.—Diagram of rig for holding salt cakes in water of lake during erosion tests. Framework holding stinger with salt cake is hinged at the boat prow, so the cake can be lifted from the water by the block and tackle attached to top of frame. Both depth and attitude of stinger are adjustable.

As the boat was driven by an outboard motor, its speed was measured by use of a water manometer on a float (pl. 9a) towed behind a light boom, well away from the bow waves of the boat. The operator read the dynamic pressure directly on the meter stick alongside the manometer, and could thus regulate the speed of the motor to maintain constant water speed. In later tests a level was used in the boat so that reproducible trim could be maintained by shifting the positions of the crew during the tests.

Tests were made on salt cakes of five different chemical compositions during the fall, winter, and spring of 1957–58 in Lake Wauberg near Gainesville. The five types were pure white salt; yellow salt containing 98 percent salt and 2 percent sulfur; a brown cake of pure salt with about 2 percent of iodine in it; a blue salt cake with a trace of copper sulfate or carbonate; and a deep red salt cake containing 2 percent of impurities including iron, manganese, copper, cobalt, and iodine. Water erosion produced results that were qualitatively much the same on all cakes, regardless of chemical composition; however, the pure salt tended to be more pitted and irregular in its erosion.

Observations

A series of runs at various speeds and lengths were made on salt cakes having various initial shapes. Plates 9–14 illustrate the results.

The salt cakes as purchased (pl. 9*b*) were rectangular blocks 12 inches long and 8 inches square, weighing 50 pounds. The depression at each end was made by the form in which the kiln-dried salt was pressed. The depression, usually saucer-shaped, was I-shaped in the iodine salt cakes. To mount a cake on the stinger, a 2-inch hole was drilled in one end of the salt cake. The stinger, fitted with a pair of soft rubber stoppers between washers at its tip, was slipped easily into the hole. The rubber stoppers were compressed by a nut, and expanded sidewise enough to hold the block firmly on the stinger.

Some runs used salt blocks shaped like that shown in plate 9*b*. Others used circular cylinders 8 inches in diameter and 10 inches long, machined from the salt blocks as purchased. Still other blocks were machined into the shape of an ogive, or pointed arch (pl. 9*c*). Machining was done on a Shop Smith, by a wood lathe technique. Various salt compositions differ considerably in ease of machining; their durability under erosion seems to bear no relation to hardness in the machining process.

The forms resulting from erosion varied greatly. White salt cakes in their original form eroded very irregularly (pl. 10*a*). Iodine salt eroded in a somewhat more orderly fashion (pl. 10*b*). A hairpin-shaped pit is clearly visible just upstream of the corner of the cake in the center of the figure (pl. 10*b*). An apparent break in the center of the pit results from the presence of another pit of the same type just above it, with a high ridge at its center just upstream of the break. Two pits near the top of the cake are in the process of fusing. The one on the left is seen in profile; its location just upstream of the corner on the left is quite analogous to the pit in the center of the figure. The neighboring pit with which it is combining is visible above the center one. Flow lines are clearly visible in each pit, running in directions normal to the pit edge, from the high point in the center. The pits shown obviously tend to erode back toward the point of the cake.

If the mechanism of pit erosion is assumed to be a hairpin-shaped vortex with axis lying in the pit, the directions of the flow lines are properly rationalized. The legs of the vortex trail downstream, as indicated by corresponding grooves that become shallower downstream. Where two pits are so near as to begin to fuse, the neighboring legs of their generating vortices should cancel out, since they would be rotations in opposite sense. The tendency to cancel is recognizable in the two fusing vortices of plate 10*b*. In the salt cakes, many pits may appear in which one leg of the vortex is altogether missing; ordinarily a canceling vortex leg can be found to account for the disappearance.

Plate 10*b* also shows many small pits on the side of the cake far from the tip. These bear a superficial resemblance to pitting on meteorites; however, that fact is not particularly significant and the pits display no recognizable erosion pattern beyond the apparent evidence of turbulence.

A striking characteristic of the iodine salt cake shown in plate 10*c* is the presence of many small pits near the tip without any easily recognizable pattern of shape or arrangement. Obviously the block is tending toward a more pointed shape than it had originally. During erosion the block was moving at a speed somewhat less than that of most of the other blocks shown in the photographs.

A more orderly and recognizable pattern of erosion than that provided by the iodine cakes was observed on cakes of blue salt (pl. 11*a*,*b*). Plate 11*a* shows an extraordinarily well developed pit with the expected hairpin shape of the generating vortex. The pit straddles the corner, but not symmetrically; the flow lines inside the pit run from the high point in the center normally to the pit edge. The right leg of the generating vortex is indicated by the groove carved on the cake on the right; the other leg of the vortex is hardly detectable. Immediately above the large pit shown, another rather similar one is visible, with less typical shape and less striking flow lines. The left leg of the pit is present as a groove not easily visible in the highlighted side on the left; the right leg is missing. On the other side of this cake are two pits, neither one straddling a corner, but located on the flat side.

Plate 11*b* shows a block of blue salt whose pitting pattern, in spite of apparent differences, resembles that of the block in plate 11*a*. The large and well-formed pits on the two corners shown in plate 11*b* have enlarged and receded toward the point of the cake so far that they are close to fusing, and about to remove the tip of the cake. The pit on the left is visible almost in profile. Both pits are far enough up on the shoulder of the cake so that the legs are not visible as grooves, although the low ridge running down on the left of the face may be a remnant. A pit is also visible in the middle of the face, somewhat downstream of the shoulder. The stagnation point at the center of the pit is a high point rather than a low one as in meteorite pits.

Before erosion, the three iodine salt cakes shown in plate 11*c* were right or flat-ended circular cylinders obtained by machining the purchased blocks. Cakes of this shape were not expected to pit during erosion. The first two samples on the left in the photograph were not carefully oriented; the third was alined with the boat axis and kept level. The deep pit just downstream of the point in the first sample is believed to have been favored by an angle of pitch in the attitude of the cake. Although the shape is not typical of those formed by a hairpin vortex, a high point occurs below the deepest part of the pit, and ridges down the side mark the location of the vortex legs. Presumably the pit was in the lee of the point, which was cocked a little with respect to the flow. The middle block has a small pit, also just downstream from the point, that shows flow lines and the typical hairpin shape. A tendency to pit is evident near the point of the third sample, but some reduction in pitting seemed to result from the care taken in maintaining the attitude of this salt cake.

A more dramatic demonstration of the influence of attitude on tendency to pit is presented in plates 12 and 13. The attitude of the blue salt cake shown in plate 12*a* (initially a right circular cylinder) was not checked or maintained, and the block is deeply pitted. The thin hook at the tip is the relic of a large pit quite similar to that near the tip of the cake in plate 11*b*, but it represents a later stage in erosion. One well-formed pit lies just downstream of that in the hook; and to the left are two overlapping "half-pits," showing only one leg of the hairpin vortex. The lack of a leg on the upper "half-pit" might be accounted for by the observation that the leg should cancel with one leg of the vortex in the hook. The absence of the left leg of the lower pit has not been explained so far. The deep pitting on the shoulder probably was favored by a chance pitching angle of the cake to the relative motion of the water.

The blue salt cake shown in plate 12*b* also started as a right circular cylinder. The axis of the cylinder was carefully adjusted to be parallel to the motion of the boat, and this attitude was maintained during the run by use of a level in the boat. It is clear that there is no trace of a pit anywhere on the surface. This result was demonstrated repeatedly by use of sulfur (pl. 12*c*) and other salt (pls. 13*a*, 14*a*) cakes whose initial shapes were right circular cylinders, ogives, and cones.

In plate 14*a*, the first two blue salt cakes on the left (shown earlier in pl. 11*a*,*b*) started as rectangular blocks. The other four were cylindrically symmetrical; only the first of these four is pitted, and it was the shape of the cake in plate 12*c*, which was presumed cocked to the flow since no effort was made to adjust its attitude. The second and third shapes from the right initially were ogives; the one at the far right was a right circular cylinder. These last three were adjusted to be straight with respect to the boat's motion.

In short, these experiments gave ample proof that pitting is completely suppressed, or at least substantially reduced, whenever the initial shape of the salt cake is cylindrically symmetrical around a line that is parallel with the direction of motion of the boat. However, even when all controllable conditions are the same there may be considerable differences in pitting. The white salt ogive on the right in plate 13*a* was not pitted, but its surface was not as regular as those of blue salt cakes subjected to the same erosion conditions.

Reference has been made to the characteristic appearance of the trailing surfaces of meteorites (p. 52). A similar appearance is characteristic also of trailing faces of salt blocks, as shown in plate 13*b*. The iodine salt cake was chosen arbitrarily from among eroded blocks having the same type of carving on the rear. The appearance, referred to as "mottled," is due to broad and shallow depressions. Notice that the edge of the face has a sharp skirt. A corresponding view of a meteorite's trailing face appears in plate 6*c*.

Pit formation in salt cakes

The photographs of eroded salt cakes in plates 10 to 14 show the following general features:

Pitting of surfaces usually occurs. The degree of pitting varies greatly, depending on the sample's material, and attitude to the fluid motion.

The detailed geometry of pit arrangement is not precisely reproducible from sample to sample. However, pits appear at a number of typical locations:

(1) In the lee of a projection such as an ogive point cocked to the water flow. (Pl. 12*a* shows one such pit in its last stage before disappearance, another example appears in the left cake in pl. 11*c*.)

(2) Upstream of projections, such as the corners of square blocks. (Examples occur in several figures, notably pl. 11*a*.)

(3) Downstream of a sharp shoulder. (Lower pit of pl. 11*b* is an example.)

(4) On a face parallel to the water flow, far from the front tip. (Pl. 10*b*.)

(5) On the base of eroding bodies. (Pl. 13*b*.)

Pitting either does not occur at all or occurs much less frequently on objects having a cylindrical symmetry around an axis parallel to the direction of water flow (pl. 14*a*). A right circular cylinder is a little less pit-resistant than an ogive. A small yawing angle causes a pit in the lee of the tip of an ogive (pls. 12, 13*a*).

The centers of the pits in salt cakes tend to show high points rather than low points. In meteorites, the flow lines suggest the presence of a hairpin-shaped vortex lying in the lee of the upstream edge of the pit, straddling a stagnation point at the deepest point of the pit. In the salt cakes exactly the same type of vortex is evident, similarly hairpin-shaped, and lying in the pit straddling the stagnation point in the pit. But since the stagnation point in salt cakes is a high point rather than a low one, it indicates a minimum rate of erosion, rather than a maximum rate at the stagnation region, as in meteorites.

The mechanism of pit-formation in salt cakes was in most cases quite recognizably a vortex. Plate 11*a* shows perhaps the most convincing evidence of the nature of the flow. The flow lines in the pit are here normal to the edge, which is so sharp as effectively to preclude serious consideration of any but vortex flow inside the pit.

The nature of water flow over the surface of the pitting cakes obviously changes with time—pits form and deepen; they may be intersected by competing pits; and they may be erased.

The same flow patterns first observed on meteorite surfaces are recognized also on the surfaces of salt cakes subjected to erosion by flowing water. It has not been determined whether differences in detail may exist due to the supersonic speed of the meteorites as compared to the low speed of the salt cakes. Since the pits in the salt were formed by vortices identified by their carving action, it seems a reasonable hypothesis that the pits on meteorites were formed similarly by vortices, identified by their flow lines in the pits.

Cavitation

The process of cavitation, often observed to effect dramatic erosion of solids in motion under water, can hardly be a factor in the experiments under discussion here. Cavitation is known to occur when dynamic pressures are of the same magnitude as the static pressure on the submerged body. Thus cavitation would be expected on an object at a depth of 1 foot of water at sea level, at speeds such that the dynamic head would be about 35 feet of water. This would be at a speed of 28 knots, larger by a factor of 6 than the speeds used in the tests.

The vortex mechanism of pit formation

The following analysis proposes to rationalize, as far as possible, the hypothesis of a vortex mechanism of pit formation in salt cakes. This hypothesis will be supported if

(a) the existence of vortices at places where pits are formed can be shown to result reasonably from the principles of fluid physics; and

(b) if it can be demonstrated that the presence of a vortex would set up a velocity distribution such as would be expected to increase the erosion rate.

The introduction of the idea of vortex motion as a phenomenon of fluid dynamics is generally credited to Helmholtz (1858) (see Durand, 1934, p. 330). He pointed out that whereas ideal fluids that can be described by a potential function possess no rotary motion, nonideal fluids in which no potential exists are found to be characterized by rotation in some parts. Rotation is consequently found in connection with flow of viscous fluids across solid surfaces.

The use of the concept of rotation in describing the lift of an airfoil is familiar. In this discussion the problem is to connect the formation of vortices with erosion, which is already presumably related in some way to drag forces on a solid in a fluid stream. The classical work on trailing vortices by von Karman (von Karman and Rubach, 1912; Durand, 1935, p. 346) extended as far as the computation of the drag on a bluff body, from the geometry of the vortex array in the wake. However, the theory was not capable of predicting the geometry of the trailing vortex array from the shape of the body (Prandtl, 1952).

The requirement in establishing the vortex mechanism of pitting is precisely to predict the conditions under which a stable vortex will form in the boundary layer of a flow near the surface of a solid body. In this discussion no theory of any great scope is developed; however, qualitative considerations are used to predict how and where vortices will form.

A subsonic flow over a curved body tends to follow the body, as is well known from theory and experiment. In this process the pressure of the potential flow outside the boundary layer will increase, and the velocity will decrease in any region where the normal to the solid surface has a component parallel to and in the same sense as the free stream velocity. It is known that the boundary layer will tend to thicken in such a region.

A flow tends to separate from a curved body with cylindrical (or spherical) symmetry in the presence of a positive pressure gradient (Green, 1937; Prandtl and Tietjens, 1934). The pressure gradient, parallel to the flow, causes deceleration and reversed flow in the boundary layer. Such a mechanism can be used to account for the trailing toroidal-type vortex anticipated in the wake of any bluff object (pls. 5*b*, 6*c*). The same assumed mechanism can be used to lead to the conclusion that no pitting is possible in regions where the curvature of the surface is small or negative, as long as pressure gradients have no component normal to the initial direction of flow. Qualitatively, the argument is that in a two-dimensional boundary layer any tendency of the flow to stop and reverse, due to a pressure gradient parallel to the two-dimensional potential flow, will at once thicken the boundary layer. This conclusion results directly from the continuity relation for two-dimensional incompressible flow: if the x- and y-components of the velocity are u and v respectively, a reduction of u along the surface in question,

$$-du = -\partial u/\partial x\, dx,$$

must result directly in an increase in the normal component of velocity. By the continuity relation for two-dimensional incompressible flow, we obtain the relation

$$-\frac{\partial u}{\partial x} = \frac{\partial v}{\partial y}.$$

The consequence of such normal motion is that the flow outside the boundary layer must be deflected outward to cause a relative increase in v_∞ and a reduction in the pressure, i.e., a decrease in $\partial p/\partial x$ which was the initial cause of the deceleration. This change would promptly erase the tendency to form a stable vortex as long as the gradient $\partial p/\partial x$ is always parallel to the two-dimensional flow.

An attempt at a mathematical description of this type of flow has been put forward as an initial value problem by Prandtl (1940). It led to the conclusion that at the point where the pressure gradient $\frac{\partial p}{\partial x} \neq 0$ there are restrictions on $\partial u/\partial x$, $\partial^2 u/\partial x^2$, and $\partial^3 u/\partial x^3$ wherever $u=0$, if $\partial u/\partial x$ is not to become infinite. Consequently, reversed flow could not be rigorously demonstrated by the analysis. This finding is suggested as supporting the conclusion that pits cannot in fact form, because vortex flow is not stable, even in the presence of a pressure gradient, as long as that gradient is parallel to the direction of flow.

Pursuing this line of thought suggests that we might avoid the difficulty encountered in this initial-value boundary-layer problem in two-dimensional flow if three-dimensional flow were assumed or if the reaction of the boundary layer on the external potential flow were considered. We might then be able to demonstrate the stability of a hairpin-shaped vortex straddling a pressure "hill" in a boundary layer even in a region where the pressure nearby tends to decrease downstream. For the present, the evidence that stable vortices occur upstream of a projection on an eroding body must remain empirical.

Some conclusions might be drawn relating to the vortex motion in a pit during erosion. The existence of a vortex inside the pit must depend on the existence of a permanent pressure gradient holding the fluid in the vortex stationary with reference to translation downstream. The equation for the x-component of the forces, i.e., in the direction of the main flow, might be derived as follows:

Suppose a vortex exists in a pit in such a way that the fluid stays in it for a period that is long, compared to the time required for fluid in the exterior flow to pass across the pit. In cross section, the vortex might appear like that sketched in figure 6. The section is made by a vertical plane parallel to the potential flow, along the axis of symmetry of the pit. The dotted line is a flow line for the fluid in the vortex. Inside the dotted line, the velocity might be assumed to vary inversely with the distance from the vortex center, as might be assumed for a vortex in general. Outside the dotted line bounding the vortex, one might assume a boundary layer in which viscous forces are predominant. The dotted perimeter might be considered to be divided into two portions. The part designated by A_0 in the figure represents the portion adjacent to a boundary layer between the vortex and the surface of the pit. The remainder of the vortex surface is adjacent to the potential flow.

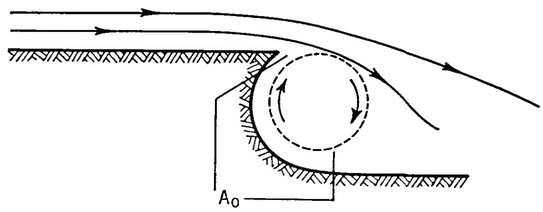

FIGURE 6.—Longitudinal section showing a vortex (dotted line) lying in a pit. Due to the flow outside the pit, there is a velocity gradient over half of the perimeter that exerts a downstream force on the vortex. Over the other half (A_0) of the perimeter the drag force between the vortex and the pit surface also is in the downstream direction. The pressure gradient balances the sum of the two viscous forces. Arrows indicate airflow; cross-hatching indicates surface.

The assumption that air stays in the vortex for a relatively long time requires that the resultant of the forces acting on the vortex—due to both the pressure gradient and the viscous drag over the vortex surface—must be equal to zero:

$$\mathbf{f}_p+\mathbf{f}_v=0.$$

Here $\mathbf{f}_p$ is the resultant of the pressure gradient forces, acting on the vortex element, and $\mathbf{f}_v$ is the resultant of the forces due to viscous drag on the vortex, i.e., due to the velocity gradients at the vortex boundary.

Suppose now that the area A_0 of the vortex is described in terms of the element of length, dz, of the vortex and that central angles α and β are measured as positive clockwise from the pole, which is parallel to the negative x-direction. The force on an element $r\,d\theta\,dz$ of area on the periphery of the vortex has a component in the x-direction given by

$$dz\,d\mathbf{f}=\mu\frac{\partial v}{\partial r}r\,d\theta\sin\theta\,dz. \tag{1}$$

The gradient $\partial v/\partial r$ is that at the boundary of the vortex at a distance r from its center. This gradient reverses direction at the points corresponding to central angles α and β, the bounds of the area A_0. It is therefore proper to write

$$\mathbf{f}_v=\int_{-\beta}^{\alpha}\mu\left(\frac{\partial v}{\partial r}\right)_1 r\sin\theta\,d\theta-\int_{\alpha}^{2\pi-\beta}\mu\left(\frac{\partial v}{\partial r}\right)_2 r\sin\theta\,d\theta. \tag{2}$$

Here $(\partial v/\partial r)_1$ is the gradient in the boundary layer between vortex and pit surface, $(\partial v/\partial r)_2$ is that in the boundary layer between vortex and external potential flow.

Suppose $(\partial v/\partial r)_1$ and $(\partial v/\partial r)_2$ have constant mean values over the respective ranges of θ in which they act. The resultant $\mathbf{f}_v$ is then computed to yield the value,

$$\mathbf{f}_v=\mu r(\cos\alpha-\cos\beta)\left\{-\left(\overline{\frac{\partial v}{\partial r}}\right)_1+\left(\overline{\frac{\partial v}{\partial r}}\right)_2\right\}. \quad (3)$$

According to the sign convention $\overline{(\partial v/\partial r)_1}$ is negative so that equation (3) represents a force downstream of magnitude

$$\mathbf{f}_v=\mu r(\cos\alpha-\cos\beta)\left\{\left|\overline{\frac{\partial v}{\partial r}}\right|_1+\left|\overline{\frac{\partial v}{\partial r}}\right|\right\}. \quad (4)$$

The equilibrium condition is then

$$2r\frac{\partial p}{\partial x}+\mu r(\cos\alpha-\cos\beta)\left\{\left|\overline{\frac{\partial v}{\partial r}}\right|_1+\left|\overline{\frac{\partial v}{\partial r}}\right|_2\right\}=0. \quad (5)$$

Equation (5) states one of the conditions necessary for a vortex to remain stationary on the surface of a solid over which fluid is flowing. Another condition is that the rotary motion of the vortex should continue for a time, t, long compared to the time for fluid in the external flow to cross the pit ($t>>2r/v_\infty$). The energy fed into the rotation of fluid in the vortex by the external flow should be equal to that absorbed by friction on the pit wall. If the energy imparted to the vortex were in the form of work done by viscous forces, and if the velocity of the fluid at the vortex boundary is assumed uniform, the energy conservation law is given by the equation

$$\mu r\left|\overline{\frac{\partial v}{\partial r}}\right|_1(\alpha+\beta)=\mu r\left|\overline{\frac{\partial v}{\partial r}}\right|_2[2\pi-(\alpha+\beta)]. \quad (6)$$

That is,

$$\left|\overline{\frac{\partial v}{\partial r}}\right|_1=\left|\overline{\frac{\partial v}{\partial r}}\right|_2\left\{\frac{2\pi}{\alpha+\beta}-1\right\}. \quad (7)$$

Brief consideration of equation (7) is sufficient to demonstrate that the model thus far developed cannot possibly account for the deepening of a pit by erosion, if the erosion rate increases with the fluid velocity. (That such an increase in fact takes place is demonstrated later; increase in erosion rate with increase in velocity is in any case a reasonable assumption.) Suppose, for example, that in equation (7), $\alpha+\beta=\pi$ radians. For such a case

$$\left|\overline{\frac{\partial v}{\partial r}}\right|_1=\left|\overline{\frac{\partial v}{\partial r}}\right|_2.$$

The erosion rate might be presumed proportional, more or less, to $|\overline{\partial v/\partial r}|_1$. But the erosion rate inside the pit must then be less than that outside the pit just upstream, where the velocity gradient is $|\overline{\partial v/\partial y}|_0$, say. For $|\overline{\partial v/\partial r}|_2$ must be less than $|\overline{\partial v/\partial y}|_0$ because $|\overline{\partial v/\partial r}|_2$ is due to a boundary layer between flows having speeds of v_∞ and $v_{\text{vortex}}\neq 0$ whereas the $|\overline{\partial v/\partial y}|_0$ is due to a boundary layer between fluid with the speed v_∞ and the wall where the speed is zero. If the boundary layers are of equal thickness inside and outside the pit, it follows that

$$\left|\overline{\frac{\partial v}{\partial r}}\right|_1<\left|\overline{\frac{\partial v}{\partial y}}\right|_0,$$

and hence the erosion rate inside the pit would be less than that outside, as was stated.

It should be emphasized that there is no assurance that the boundary layers have equal thicknesses inside and outside the pit. Hence the question as to how large the velocity gradients may be in various boundary layers cannot be answered at present.

An alternative viewpoint relating to the conservation law for energy may be somewhat more promising for rationalizing the observations. Consider the following argument: In the analysis thus far made, no account has been taken of the continuity relation. It has been suggested in the preceding discussion that to apply that relation to the case under discussion would require some flow normal to the plane of the section shown in figure 6; that is, fluid is continually fed into the pit from the boundary layer upstream. In order that the vortex should remain constant in size, there must be a continuous outward flow of fluid in a direction normal to the section of vortex considered. If the boundary layer upstream has a depth δ and a mean velocity $v_\infty/2$, the mass flow into the vortex would be $\rho v_\infty\ \delta dz/2$ where ρ is the fluid density. This must be equal to the net outward flow of fluid, $2\pi r^2 \rho w \times 2$ where w is the outward axial flow at distance $dz/2$ from the plane of figure 6. That is,

$$\frac{v_\infty \delta\, dz}{2} = 2\pi r^2 w \times 2.$$

It is not difficult to work up an expression based on the force law relating w with the axial component of pressure gradient. However, this discussion intends rather to draw some qualitative conclusions relating to the energy of fluid circulation inside the vortex. The model here described, of course, has more than a passing resemblance to the so-called vortex or Hilsch tube (see Scheper, 1951, for a discussion of the characteristics of the Hilsch tube). That is, fluid is fed into a vortex from the periphery with some kinetic energy and, hence, some moment of momentum; fluid is removed along the axis, or at least in the axial direction. In such a vortex tube there may be a redistribution of energy such that the energy relation of equation (7) is not valid. It is possible that the deepening of pits in erosion may be shown to be reasonable by virtue of that redistribution, in contrast with the conclusions based on the equation.

Rotational energy in a vortex

The literature dealing with analysis of flow in vortex tubes has been concerned mainly with heat flow or the separation of gases (Pohlhausen, 1921; Elser and Hoch, 1951). It is not intended at this point to discuss those characteristics of the vortex tube or to derive the dynamic characteristics of the device. However, the qualitative picture of vortex flow in a vortex tube suggests a mechanism capable of accounting for pit formation by vortices.

Consider a vortex in which the circulation is constant. Such a flow is a reasonable first approximation to a real vortex, and is characteristic of a frictionless fluid. In such a vortex, the tangential velocity v at each point is inversely proportional to the distance r of the point from the vortex center:

$$v = \frac{\Gamma}{2\pi r}. \tag{8}$$

Here Γ is the constant circulation. For such a vortex in a perfect fluid, the gradient of the tangential velocity increases inversely with r^2, as shown by the relation

$$\frac{dv}{dt} = -\frac{\Gamma}{2\pi r^2}. \tag{8a}$$

If a vortex exists in a gas having a small viscosity, the flow will tend to depart from the pattern of a free vortex. In effect, the inner layers would tend to do work on the outer layers of fluid; the velocity gradients would tend to decrease. In time the vortex would change toward the state in which the angular velocity v/r is constant.

Suppose that fluid is brought into the vortex with a rotation Γ, and that it stays for a while, being removed from the vortex axially. For some period of operation with this type of flow, the fluid should have less vorticity as it leaves than it had as it entered, vorticity being defined as the product $2\pi\, vr$. In other words, vorticity, according to this picture, should tend to accumulate in the vortex until the velocity at the periphery of the vortex is as great as or even greater than that of the fluid entering the vortex.

This behavior of fluids may be observed in the manner of operation of the cyclone separator for removing dust from air. It can be observed also in the bath tub when the water is running out the drain. And it would appear that the thermal phenomena in the Hilsch tube might be explained by use of the same model. Since a detailed analysis of the mechanism as it applies to the pitting phenomenon has not been made, the model is proposed at this time only as a possible means of rationalizing the observation that pits do form where vortices are found. That is, if an accumulation of vorticity can be demonstrated in a pit vortex, the requisite mechanism for rationalizing pit formation would be established, subject only to the further condition that the rate of erosion increase with speed of the fluid.

Variation of erosion rate

The dependence of the rate of erosion on flow speed is not difficult to demonstrate. Several series of runs were made in which the time and speed were observed as they affect the weight loss of salt cakes.

It is to be expected that erosion of a body subject to fluid flow would be proportional to the surface area exposed to the flow. That is,

$$-\frac{dm}{\rho dt}=kA, \tag{9}$$

where m is the mass of the eroded body, A is its surface area, k is the linear rate of erosion per unit time and per unit exposed area, and ρ is the density of the solid.

Suppose the shape is not greatly changed as erosion proceeds; that is, suppose $m/\rho=ar^3$, $A=br^2$, where a and b are constants, and r is some characteristic dimension of the body. Then

$$A=b\left(\frac{m}{\rho a}\right)^{2/3}, \tag{10}$$

and equation (9) yields the value

$$-\frac{dm}{\rho dt}=kb\left(\frac{m}{\rho a}\right)^{2/3}. \tag{11}$$

This equation may be integrated to yield

$$-3m^{1/3}=\frac{\rho kb}{(\rho a)^{2/3}}\,t+\text{constant}. \tag{11a}$$

If t is measured from the time when $m=m_0$, the equation can be written as

$$m_0^{1/3}-m^{1/3}=\frac{\rho kb}{3(\rho a)^{2/3}}\,t \tag{11b}$$

or

$$\left(\frac{m}{m_0}\right)^{1/3}=1-\frac{\rho kb}{3(\rho a)^{2/3}m_0^{1/3}}\,t. \tag{12}$$

Equation (12) states that the ratio of salt cake weight at any time t to its initial weight, raised to the $1/3$ power, is a linear function of time, the slope being proportional to the linear erosion rate k, and inversely proportional to the $1/3$ power of the initial weight. It should be noticed that shape factors also enter into the slope.

If the eroded body changes in shape with time, the slope of the erosion curve as derived should also change with time. However the form in which the data are presented might reasonably still be a plot of $(m/m_0)^{1/3}$ as a function of time.

Figure 7*a* presents a graph showing how the rate of erosion of two blue salt cakes varied with time of running; the relative mass to the one-third power is considered proportional to the linear size. One cake was originally an ogive; its data are well represented by a straight line throughout the experiment. The other cake was a right circular cylinder, whose data may also be represented by a straight line except for the first 6 minutes of running time, when the erosion rate was relatively small. The slopes of the two lines are equal, but the significance of that fact is not clear, because of the difference in original shape and size of the blocks. The final shapes of the two blocks, after erosion, are found in plate 14*a*, on the extreme right; they are remarkably similar in shape, and quite free of pits.

Figure 7*b* shows a set of curves representing the data on erosion of three right circular cylinders of salt cakes of different compositions. The curves are rather close together, and all three are well represented by straight lines throughout most of the running time. During the first six minutes, the blue cake was relatively more durable; the sulfur cake was slightly less so, and the iodine cake was the least durable of the three.

At 3-minute intervals during erosion, successive changes in the shape of a right circular cylinder of blue salt occur (fig. 8). Clearly the leading face of the cylinder is first rounded. The shape becomes somewhat bulbous for a period, but later the typical ogive is formed. In many salt cakes, large pits were formed throughout the run, generally on the shoulder and near the tip. None appeared on the blue cake.

These preliminary data are presented as a background for the data on erosion rate as a function of the water speed. Two series of tests were made in which salt cakes shaped as purchased (pl. 9*b*) were subjected to erosion at different speeds. That the erosion rate increases with speed is immediately made clear by a glance at plate 14*b*, showing four iodine salt cakes which were eroded for 16 minutes at different speeds. The differences in size of the cakes are clear and direct evidence, albeit not very quantitative, that erosion rate increases with water speed.

A more quantitative measure of the erosion rate would be the slope of the curve of $(m/m_0)^{1/3}$ against t, a slope presumably proportional to

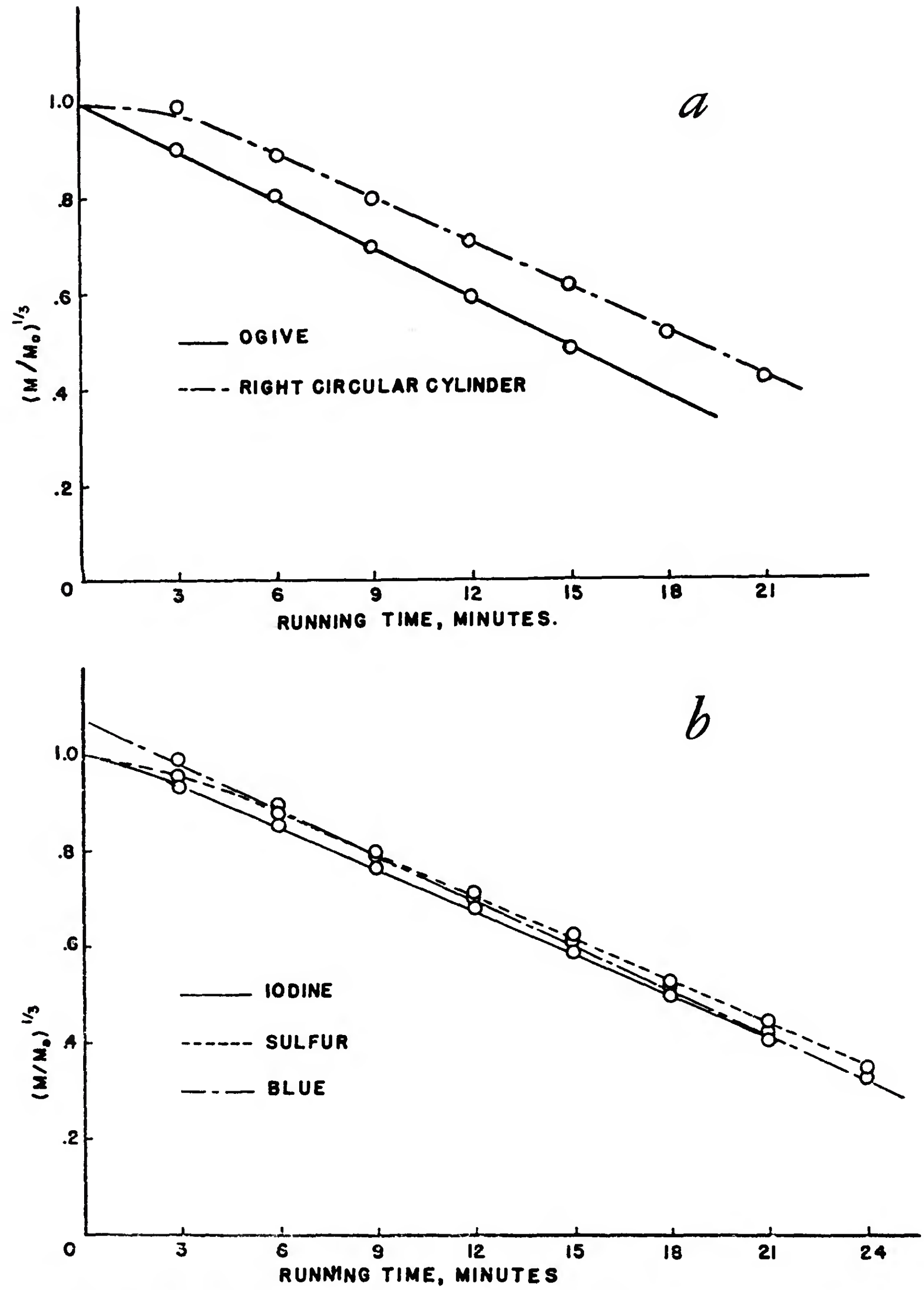

FIGURE 7.—Erosion as a function of running time; water speed, 4.8 knots. One-third power of cake weight is considered proportional to the linear size; presumably, the slopes of these curves are proportional to the linear erosion rate. *a*, Ogive and right circular cylinder, blue salt cakes. *b*, Right circular cylinders, salt cakes of various compositions.

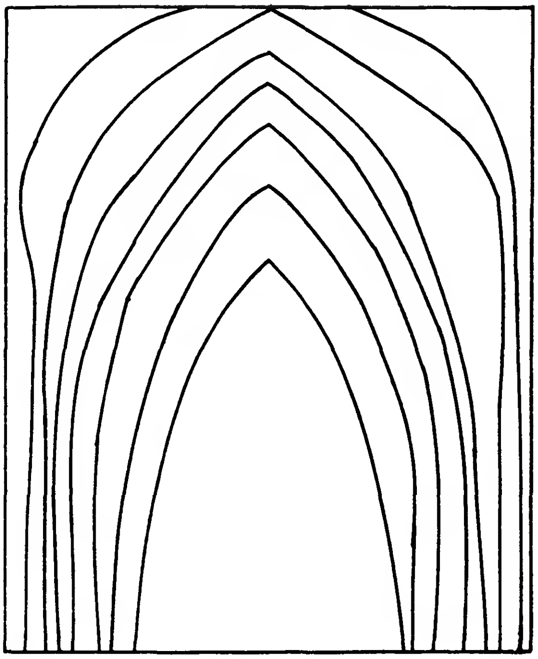

FIGURE 8.—Successive shapes at 3-minute intervals of a blue salt cylinder during erosion. Erosion begins as a rounding of the cylinder edge. A tendency to form a bulbous shape quickly gives way to the typical ogive shape. Erosion of base proceeds relatively slowly.

the linear erosion rate k (see equation (12)). The slopes for the iodine salt cake tests were computed from the initial and final weights for the four iodine salt cakes shown in plate 14*b* that were eroded at different water speeds. The results, in the form of two different curves, are presented in figure 9. The solid curve shows $\rho kb/3(\rho a)^{2/3}m_0^{1/3}$ as a function of speed; the dashed curve shows the same quantity as a function of dynamic head. Both curves are valid measures of the relative erosion rate as a function of water speed, because the composition, original shape, and original size were the same for the four blocks of iodine salt. The linear erosion rate, as measured, clearly varies as a smooth function of speed. When dynamic head is used as the independent variable, the points lie on a straight line which has an intercept above the time axis. Such a variation implies an erosion rate at zero speed, and an additional rate proportional to the square of the water speed.

Pitting of salt cakes and meteorites

The experiments on salt cakes were designed to show that the bound vortex mechanism of pit formation, as first suggested by the flow marks on meteorites, does actually operate to produce pits on eroding salt cakes; and hence, presumably, on any ablating solid body. The tests established empirically that salt cakes are pitted, exactly as predicted. The shapes and locations of the pits support the conclusion that bound vortices are responsible for the erosion. A possible mechanism was suggested which might cause higher velocity gradients in pits than in the area nearby outside the pits. Although the existence of this mechanism was not established by any complete theory, the tests provide experimental proof that an increased erosion rate in the pits would result if higher velocity gradients do exist inside the pits.

None of this evidence is, strictly speaking, a "proof"; and of course a rigorous proof is out of the question since no tests can be made on the pitting of meteorites during astroballistic flight. It is considered desirable to marshall the empirical evidence as it stands:

(a) Direct observation has proved that vortices of the same type as are detected on salt cakes in water existed on meteorites during a period when airflow was hot enough to melt them.

(b) Pits occur on meteorites at points that are altogether analogous to the position of pits on salt cake. Specifically:

(1) A meteorite like the Lafayette, which is symmetrical enough to show no pressure gradients transverse to the airflow, did not pit; similarly, the axially symmetrical salt cakes showed a reduced tendency to pit (pls. 5*a*, 12*b*).

(2) Pits are found on and near the shoulders of axially nonsymmetrical meteorites; similarly, they are found on and near the shoulders of axially nonsymmetrical salt cakes (pls. 8, 11*a*).

(3) On trailing faces of meteorites the pits bear a striking visual resemblance to those on the trailing faces of eroded salt blocks (pls. 6*c*, 13*b*).

(4) Small pits on the sides of salt cakes far from the leading face resemble meteorite pits seen on many meteorites. (Data supporting this point are not presented in any detail here, but see pls. 7*c*, 10*b*.)

(c) An increased erosion rate for salt cakes due to higher water speeds was experimentally established. If the mechanisms of pitting on meteorites and on salt cakes are similarly affected by fluid dynamic influences, presumably the effect of increased velocity in the

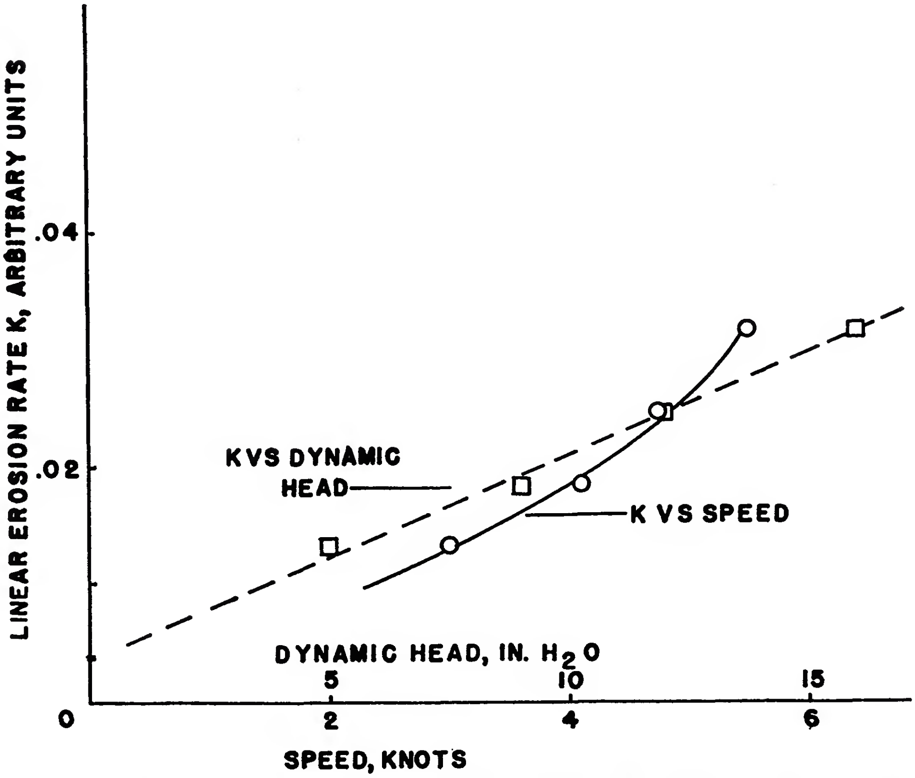

FIGURE 9.—Variation of linear erosion rate of iodine salt cake with water speed. Dashed line shows curve of linear erosion rate as a function of dynamic head. Since this line is straight, it indicates a variation proportional to the speed squared. The intercept of this line suggests that erosion would occur at zero speed.

boundary layer on erosion rate should be at least qualitatively similar for meteorites and salt cakes. That is, the erosion rate could be expected to increase with fluid speed on bodies ablating in a hot air blast, a fact that has been generally observed. To give one of many possible examples: a plate of refractory material was highly resistant to erosion when heated by a gas-oxygen torch for several tens of seconds. The same material tested in a hydrogen-peroxide kerosene rocket eroded to a depth of about an inch in somewhat less than 2 seconds. The difficulties encountered in the search for lining materials for rocket nozzles and jet vanes are well known. Thus the dependence of erosion rate on fluid speed, which is observed on salt cakes in water, is the same qualitatively as that observed for solids subject to aerothermodynamic ablation.

The evidence just summarized has convinced this author that pitting on meteorites is caused by the fluid dynamic mechanism of bound vortices. It should be pointed out that this conclusion is not affected in any way by the following facts:

(a) The detailed processes involved in erosion on salt cakes and on meteorites are quite different.

(b) The meteorites were subject to supersonic flow, and the salt cakes to subsonic flow.

(c) The materials, sizes, and Reynolds numbers of the flows over meteorites and over salt cakes are different.

(d) The detailed dependence of erosion rate on fluid speed presumably differs in meteorites and in salt cakes.

(e) As far as any conclusions drawn here are concerned, erosion and possibly pitting of meteorites might also be effected without the presence of vortices, or even in the absence of enough air to form a shock wave. That is, no assertion is made here that all pits in meteorites are due to vortices.

The arguments summarized here have led the author to conclude also that pitting of the same type may be studied on erosion models subjected to subsonic flows. The model chosen for the research presented here is, of course, not the only one possible. Specifically, the conclusions reached here might be supported by detailed measurement of flow speeds inside such pits as are actually formed by water erosion. A hot wire anemometer could be used in a low-speed wind tunnel to test salt cakes previously pitted in the manner described in this paper. The same type of study might be made also of plaster casts of meteorites. Such a program of studies might greatly advance the detailed theory of ablation and pitting of coatings for vehicles designed for reentry from outer space.

The type of study suggested here, of course, is not at all new, though the application to pitting may be. Work reported by Berman (1955) presents a theory that would be useful in developing a proper analogy between ablation and heat transfer. The experimental study that served as a background for that work was the ablation of icicles in a wind tunnel.

References

ALLEN, W. A., AND MAYFIELD, E. B.
1953. Journ. Appl. Phys., vol. 24, p. 131.
ALLEN, W. A.; RINEHART, J. S.; AND WHITE, W. C.
1952. Journ. Appl. Phys., vol. 23, p. 132.
BERMAN, K.
1955. Journ. Appl. Mech., vol. 22, p. 196.
COOK, A. F.
1954. Astrophys. Journ., vol. 120, p. 572.
COOK, A. F., AND MILLMAN, P. M.
1955. Astrophys. Journ., vol. 121, p. 250.
COOK, M. A.; EYRING, H.; AND THOMAS, R. N.
1951. Astrophys. Journ., vol. 113, p. 475.
DURAND, W. F.
1934. Aerodynamic theory. Vol. 1, 398 pp.
1935. Aerodynamic theory. Vol. 2, 367 pp.
ELSER, K., AND HOCH, M.
1951. Zeitschr. Naturf., vol. 6a, p. 25.
FALES, E. N.
1926. Visible study of flow. McCook Field Rep., Serial No. 2635. Published by Chief of Air Service, Washington, D.C.
GREEN, S. L.
1937. Hydro- and aeromechanics. 166 pp.
HELMHOLTZ, H.
1858. Journ. Reine Angew. Math., vol. 55, p. 25.
HENDERSON, E. P.
1958. Proc. U.S. Nat. Museum, vol. 107, p. 339.
HENDERSON, E. P., AND WILLIAMS, D. T.
1958. Techn. Rep. No. 9, Smithsonian Inst. Astrophys. Obs.
JACCHIA, L. G.
1955. Astrophys. Journ., vol. 121, p. 521.
NININGER, H. H.
1936a. Amer. Journ. Sci., vol. 31, p. 209.
1936b. Amer. Journ. Sci., vol. 32, p. 1.
1952. Out of the Sky. 336 pp.
POHLHAUSEN, E.
1921. Zeitschr. Angew. Math. Mech., vol. 1, p. 115.
PRANDTL, L.
1940. Tech. Mem. No. 959, National Advisory Committee for Aeronautics.
1952. Essentials of fluid dynamics. 452 pp.
PRANDTL, L., AND TIETJENS, O. G.
1934. Applied hydro- and aeromechanics. 311 pp.
RIABOUCHINSKY, D.
1909. Bull. Inst. Aérodyn., Koutchino, vol. 3, p. 59.
RINEHART, J. S.
1957. Bull. Amer. Phys. Soc., ser. 2, vol. 2, p. 45.
RINEHART, J. S.; ALLEN, W. A.; AND WHITE, W. C.
1952. Journ. Appl. Phys., vol. 23, p. 297.
SCHEPER. G. W., JR.
1951. Refrig. Eng., vol. 59, p. 985.
SMITH, H. J.
1954. Astrophys. Journ., vol. 119, p. 438.
THOMAS, R. N.
1952. Astrophys. Journ., vol. 116, p. 203.
THOMAS, R. N., AND WHIPPLE, F. L.
1951. Astrophys. Journ., vol. 114, p. 448.
THOMAS, R. N., AND WHITE, W. C.
1953. Astrophys. Journ., vol. 118, p. 555.
VON KARMAN, T., AND RUBACH, H.
1912. Phys. Zeitschr., vol. 13, p. 49.
WHIPPLE, F. L.
1943. Rev. Mod. Phys., vol. 15, p. 246.
1955. Astrophys. Journ., vol. 121, p. 241.
WHIPPLE, F. L., AND THOMAS, R. N.
1951. Journ. Aeron. Sci., vol. 18, p. 636.
WHITE, W. C.
1955. Astrophys. Journ., vol. 121, p. 271.
WHITE, W. C.; RINEHART, J. S.; AND ALLEN, W. A.
1952. Journ. Appl. Phys., vol. 23, p. 198.

Abstract

Flow lines on meteorites were photographed to determine the nature of airflow inside the "thumb pits" in the surface. The flow is shown to be consistent with that occurring if a hairpin-shaped vortex were lying with bent portion in the pits, with vortex legs trailing off to infinity downstream. Since such a flow is not unique to supersonic fluid speeds, the prediction is made that pits similar to those on meteorites would be observed on salt cakes pushed through a lake. Experiments demonstrated that salt cake erosion may indeed be accompanied by pit formation due to vortices precisely like those detected in meteorite pits. The evidence, supplied by photographs, leads to the conclusion that pitting is a general phenomenon in eroding fluid flow, and that tests at low speeds may provide valuable information regarding certain problems in astroballistic ablation.

U. S. GOVERNMENT PRINTING OFFICE: 1959

Erosion pattern carved in a ceramic plate by a rocket blast, with evidence of reversed flow at the bottom. As the blast "bounced" along the surface, it created vortices in the boundary layer between the plate and the blast.

499091—59——3

a, Enlargement of region "b" of text figure 1, showing reversed flow just upstream of point of impingement of rocket blast. Flow direction is marked by a streamer of glass terminating in a knob formed by surface tension.

b, Enlargement of region "C" of text figure 1, showing crest region above the plate surface. Main flow, marked by glass streamers, is upward and toward the left.

Enlargement of a crest region in the eroded ceramic plate pictured in plates 1 and 2. The main flow is upward. Due to a vortex in the boundary layer the flow in the lee of the crest is roughly at right angles to the main flow, as indicated by the glass rivulets terminating in a knob.

Estherville oriented iron meteorites. All photos same scale.

a, Stagnation point is in the center. Airflow was upward. Flow lines appear in the oxide layer, which has broken off near the top, showing the smooth iron beneath.

b, Stagnation point is at bottom. Airflow was upward. Flow lines on the oxide layer are finer than the carved features in the once molten iron.

c, Stagnation point is at bottom. Airflow was upward. Oxide crust has broken off near the top.

a, Leading face of the Lafayette stone, with stagnation region near the bottom. The airflow, smooth and producing no pitting, is clearly marked by flow lines. Flow left the stone where the top edge of the face is marked by a skirt of slag.

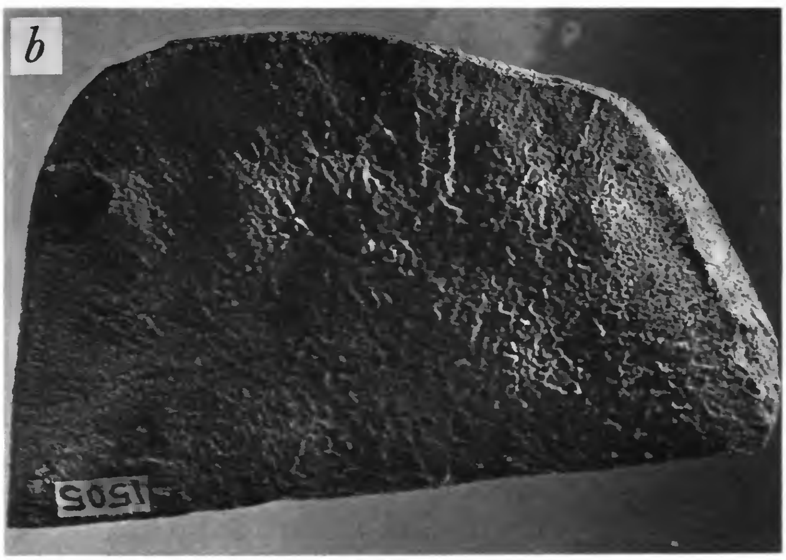

b, Trailing face of the Lafayette stone, with stagnation point at lower center. Flow outward toward the edge is indicated by a skirt of slag, where airflow left the stone.

a

a, Leading face. Flow lines diverge from stagnation point, just left of center. Pits on right show flow lines inside.

b

b, Side 3 (text fig. 3*a*), full face view. Front face is at bottom. Airflow was upward. Flow lines are visible inside all pits, but vortices not evident.

c

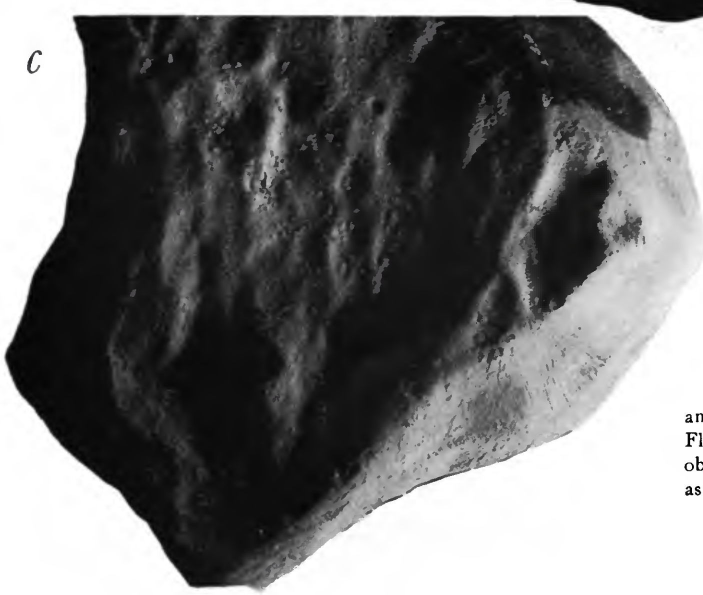

c, Trailing face. Characteristic mottled appearance is caused by broad, shallow pits in surface. Flow lines radiate from center. A distinct skirt is observable only on edge to the left and as far around as the point at the bottom.

Faces of the Plainview, Tex., meteorite (No. 521). This stone is flat on front and rear.

a, Side 5 (text fig. 3*a*) of Plainview meteorite, with stagnation region toward the bottom.

a

b

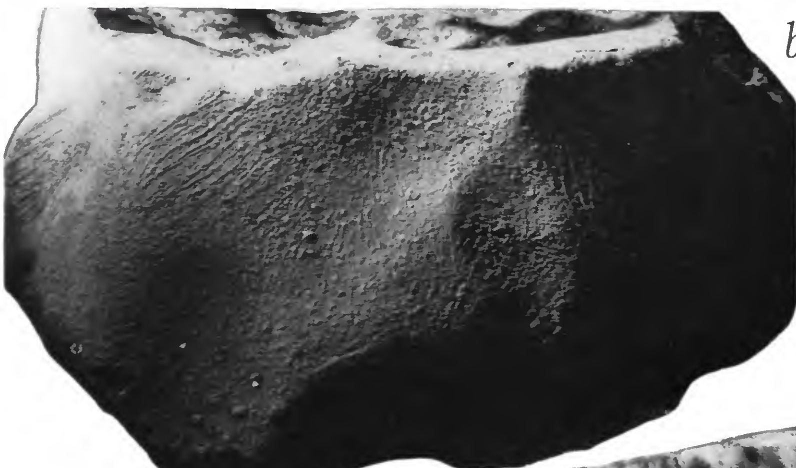

b, Region 6 (text fig. 3*a*) of Plainview meteorite. This face is adjacent to side 5, on the left; the trailing face is toward the top, the leading face toward the bottom.

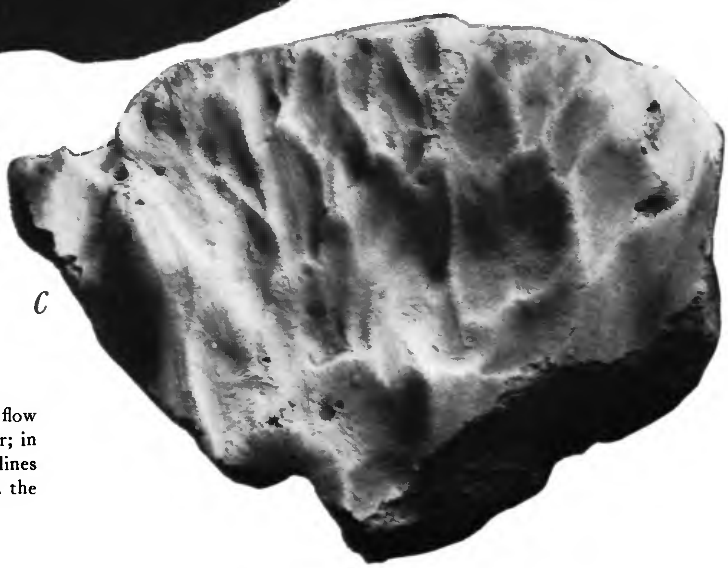

c

c, The Olivenza fragment. The flow lines inside the pits are unusually clear; in each pit is a stagnation point with flow lines diverging more or less directly toward the edges.

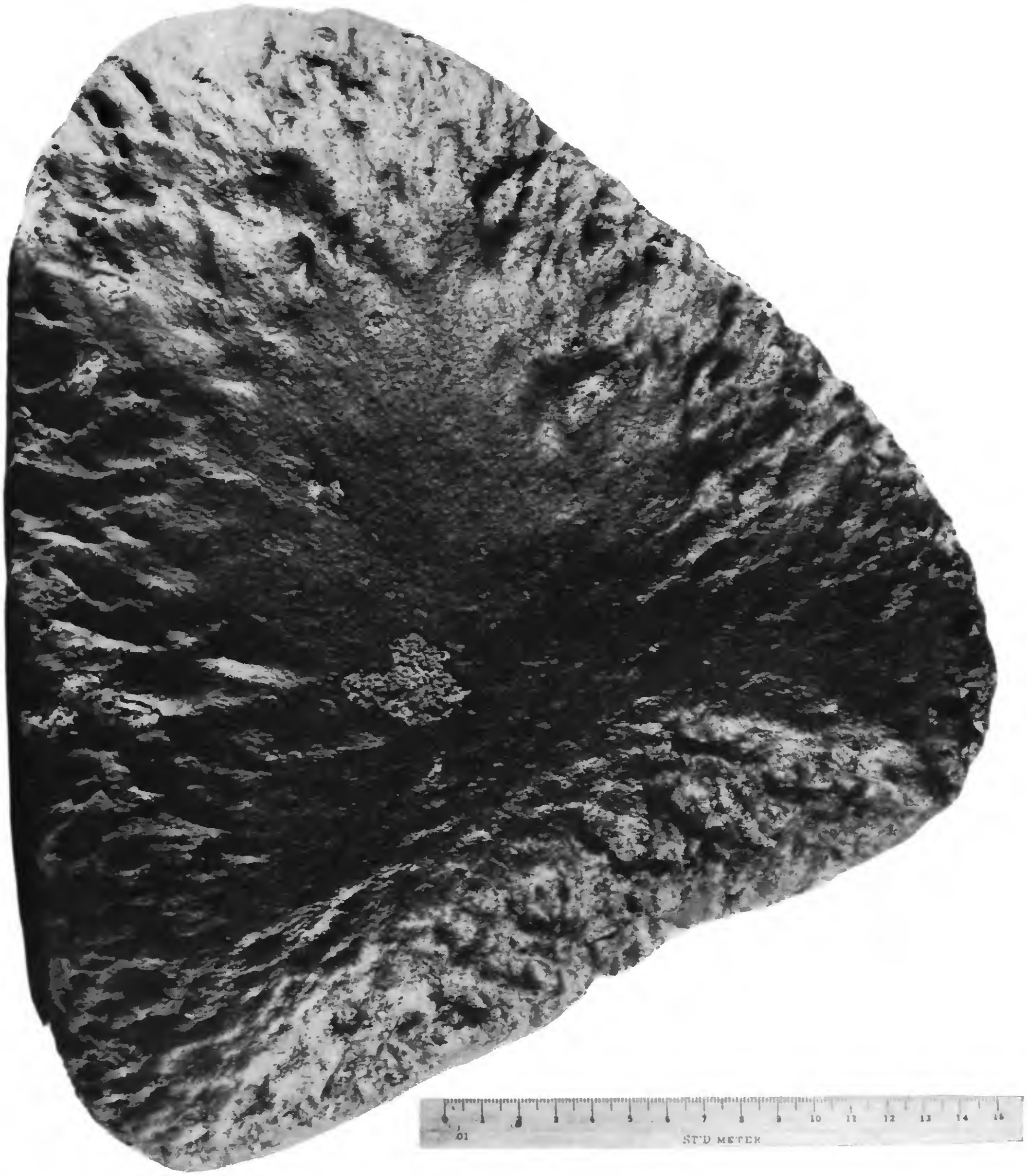

Leading face of the Miller meteorite, with the stagnation region at the center. Note radial orientation of the pits on the shoulder.

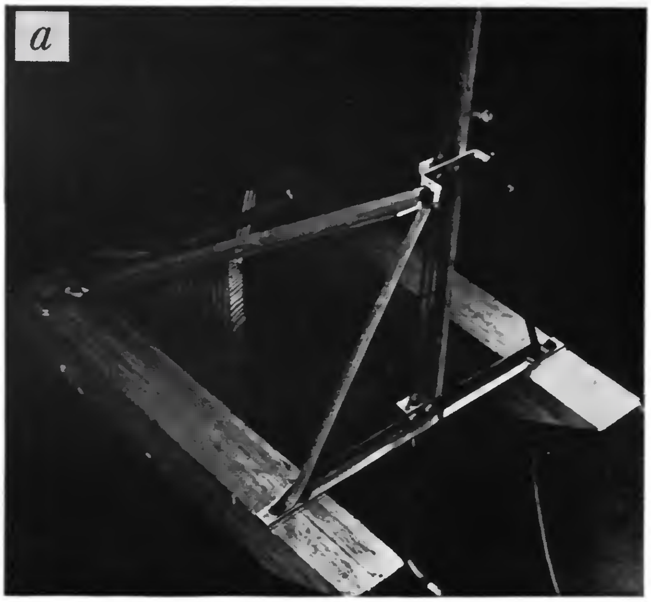

a, Speedometer used when towing salt cakes.

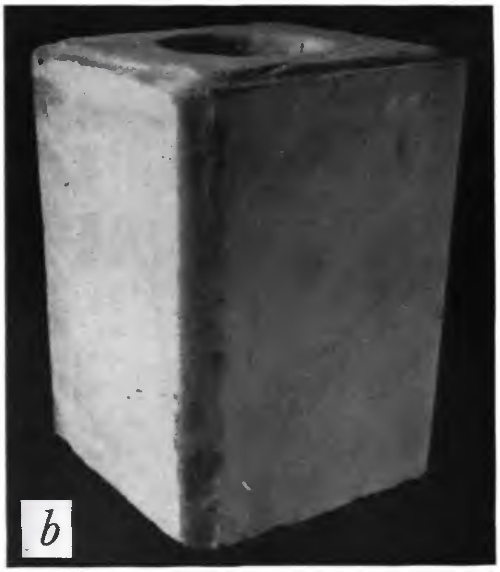

b, Salt block as purchased.

c, Ogive machined from salt block (*b*).

a, White salt block after erosion for 8 minutes at 4.1 knots, showing irregular erosion and deep pitting. Eroded shapes are so intricate that interpretation of water flow is difficult.

b, Iodine salt block after erosion for 8 minutes at 4.1 knots. Note orderly pit system on the leading end and the small pits near the base, far from the tip.

c, Iodine salt block after erosion for 16 minutes at 3.1 knots. Pitting is extensive on the leading face, a characteristic of low speed erosion on bluff objects.

a, Blue salt block after continuous run for 16 minutes at 4.8 knots.

b, Blue salt cake after intermittent run for 16 minutes at 4.8 knots. The run was intermittent to permit successive weighings.

c, Iodine salt cakes (initially right circular cylinders) after erosion at 4.8 knots for (left to right) 18 minutes, intermittent; 16 minutes, steady; and 21 minutes, intermittent.

a, Blue salt cake (initially a right circular cylinder) after erosion at 4.8 knots for 16 minutes with attitude not adjusted.

b, Blue salt cake (initially a right circular cylinder) after erosion at 4.8 knots for 21 minutes with attitude adjusted.

c, Sulfur cakes after erosion at 4.8 knots. First two cakes (initially rectangular blocks) ran 16 minutes; the third (initially a right circular cylinder) and fourth (initially an ogive) ran 12 minutes. Only the fourth cake, the only one with attitude adjusted, shows no pitting.

a, White salt cakes (initially symmetrical) after erosion at 4.8 knots for (left to right) 14, 14, 8, and 12 minutes. The first block on the left was the only one not adjusted as to attitude. The first two cakes on the left were right circular cylinders; the other two were ogives.

b, Base of an iodine salt cake after erosion at 5.5 knots for 16 minutes, typical of all base areas on eroded bodies. Note the broad and shallow depressions and striking resemblance to meteorite trailing faces.

a, Blue salt cakes after erosion at different lengths of time and speeds. Only the three unpitted shapes on the right were both symmetrical initially and adjusted as to attitude; of these, the cake at the far right was a right circular cylinder and the other two were ogives. The difference in color of the cake furthest right suggests variation in composition.

b, Iodine salt cakes (initially rectangular blocks) after 16 minutes at (left to right) 3.1, 4.1, 4.8, and 5.5 knots.